Denoising for Diffusion Tensor Imaging of the Human Brain with High Spatial Resolution

K. R. Hahn[1], S. Prigarin[2] , K. Rodenacker[1], K. M. Hasan[3]

[1] Institute of Biomathematics & Biometry, Helmholtz Zentrum München,
German Research Center for Environment and Health, Neuherberg, Germany
[2] Institute of Computational Mathematics and Mathematical Geophysics, Novosibirsk, Russia
[3]Department of Diagnostic and Interventional Imaging, University Texas, Houston, USA

Abstract— **A denoising method for Diffusion Tensor Imaging is proposed, with the aim to reduce the presently used clinical voxelsize of 8 ~ 27 mm^3 to approximately 1 mm^3. The method combines voxelwise averaging, nonlinear filtering and Rician bias correction of the directly measured Diffusion Weighted Images. To eliminate residual noise, a final postfiltering procedure applied to DTI quantities is performed. The method is based on the Delta Method formalizing the asymptotic Gaussian limit of nonlinear noise propagation. The method is explored via Monte Carlo simulations on human brain data measured with 1x1x1 mm^3 resolution. The numerical results indicate the feasibility of quantitative analysis of Diffusion Tensor data of the human brain with 1 mm^3 resolution, measured with clinical scanning parameters, under the assumption that thermal noise effects are the dominating artifacts.**

Keywords— **Medical Image Processing, Diffusion Tensor Imaging of the Human Brain with High Resolution, Denoising of Human Brain Diffusion Tensor data with 1 mm^3 Resolution.**

I. Introduction

Diffusion Tensor Imaging (DTI) enables the in vivo characterization of nerve fibers in the human brain indicating structural lesions caused e.g. by Multiple Sclerosis or Alzheimer [1, 2]. A major limitation of DTI is its restriction to voxel-averaged quantities, where the voxelsize is large compared to the scale of the course of nerve fibers. This introduces systematic errors in scalar and vectorial nerve fiber information [3]. On the other hand, reducing voxel size lowers the signal to noise ratio (SNR) in the measured Diffusion weighted images (DWI), producing in nonlinearly derived DTI quantities non-Gaussian bias and variability.

Denoising methods of DTI data with low SNR are - to our knowledge – published in only few papers, see e.g. [4] Basu et al. 2006 and [5] Fillard et al. 2006. The main problem addressed there is the strong influence of the Rician mean value bias in the DWIs. By Zhang et al. 2008 [6] the Rician noise model is incorporated into a multi-channel wavelet-based denoising method. Martin-Fernandez et al. 2008 [7] apply a multichannel Wiener filter with Rician bias correction to the DWIs. In all approaches inclusion of the Rician noise model improves the results for low SNR DTI compared to those calculated under the assumption of unbiased Gaussian noise. Similar results were published by Hahn et al. 2005 [8], where our first approach to the denoising problem of low SNR DTI was presented. In the following we present a novel, improved method, see [9] for a more detailed report. The method combines voxelwise averaging, nonlinear filtering and Rician bias correction of the DWIs. These denoising steps reduce the main part of the noise effects, but due to sample size restrictions residual noise effects may remain. Therefore, a final postfiltering procedure of DTI quantities is performed. The method is based on the statistical Delta Method formalizing the asymptotic Gaussian limit of nonlinear noise propagation. The method is explored by Monte Carlo simulations on human data measured with 1x1x1 mm^3 resolution. The results indicate the feasibility of quantitative analysis of DTI data of the human brain with 1 mm^3 resolution, measured at a clinical field strength of 3 Tesla, with a b-value of ~ 1000 s/mm^2 and with only NEX= 4-8 replications of the basic DWI-measurements. The method is not limited to the standard tensor model, but can be applied to any diffusion model based on DWIs.

II. Materials and methods

A. Statistical aspects

Neglecting the influence of non-thermal noise, caused by scanner instabilities, patient motion or cardiac pulsation, a simplified stochastic model of noise in DTI can be formulated [9]. For this model, an illustration of nonlinear noise propagation in DTI and of our denoising strategy is given in Fig.1. Distributions for FA, a well known scalar measure of anisotropy [3], in a single voxel are derived from Monte Carlo simulations with a minimal SNR ≈ 1 in the DWIs.

O. Dössel and W.C. Schlegel (Eds.): WC 2009, IFMBE Proceedings 25/IV, pp. 744–747, 2009.
www.springerlink.com

Without DWI averaging skewness and a heavy tail is apparent, see distribution a). A high risk to draw an outlier is evident. DWI averaging of NEX=20 replications introduces an approximate Gaussian shape but also a bias b). Application of a bias correction (BC) to the DWIs produces a less perfect Gaussian shape but eliminates the mean value bias, see c). It is clear from the Figure that c) is best suited to estimate the true FA value (vertical bar) drawing a random number. The goal of the proposed denoising method is to achieve distributions like c) for all relevant DTI quantitites. The distribution c) can be further narrowed and comes closer to Gaussian shape if more replications in the DWIs are applied or if, by a final denoising step, samples of c) are averaged to replace c) by its mean value distribution (postfiltering). The properties of the distributions in Fig. 1 are in line with the statistical Delta Method (DM). The DM predicts approximate Gaussian statistics for the nonlinear derived DTI quantitites, if noise effects in the DWIs are sufficiently reduced [9].

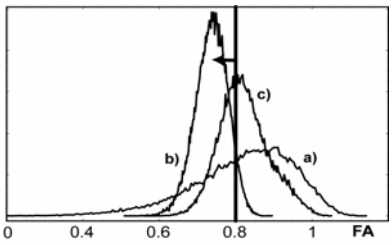

Fig. 1 FA distributions for low SNR. DWI averaging with NEX=1, a) and NEX=20, b). For distribution c) an additional bias correction is performed. Vertical bar gives the true FA value, the arrow indicates the bias shift of the mean for b); the mean value of c) is practically unbiased.

B. The spatial filter

We adapt a filter chain proposed originally by Aurich [10] to denoise DWI images with low SNR. For a first estimation we iterate nonlinear filters which calculate weighted averages of noisy scalar images $f(\mathbf{x}) = \mathrm{DWI}(\mathbf{x})$ on a grid in space, $\mathbf{x} \in \mathbf{R}^3$, within regions or scales defined by spatial and functional Gaussian windows, Φ and Ψ. The window parameters μ, η control the properties of the filter. Assuming a simplified Gaussian noise model, a constant noise level μ can be deduced from the data. The first iteration of the filter $F(\eta, \mu, \cdot)$ is defined by

$$F(\eta_{(1)}, \mu_{(1)}, f(\mathbf{x})) = \sum_{\mathbf{y} \in \textit{Neighborhood of } \mathbf{x}} \Phi\Psi f(\mathbf{y}) \; / \sum_{\mathbf{y} \in \textit{Neighborhood of } \mathbf{x}} \Phi\Psi$$

with $\Phi = e^{-(\mathbf{x}-\mathbf{y})^2/2\eta_{(1)}^2}$ and $\Psi = e^{-(f(\mathbf{x})-f(\mathbf{y}))^2/2\mu_{(1)}^2}$

For (k-1) iterations we define

$$f_{k-1}(\mathbf{x}) = F(\eta_{(k-1)}, \mu_{(k-1)}, ..., F(\eta_{(2)}, \mu_{(2)}, F(\eta_{(1)}, \mu_{(1)}, f(\mathbf{x}))))$$

The last, k-th, iteration is defined by

$$f_{smooth}(\mathbf{x}) = F(\eta_{(k)}, \mu_{(k)}, f(\mathbf{x})), \quad \text{where}$$

$$\Phi = e^{-(\mathbf{x}-\mathbf{y})^2/2\eta_{(k)}^2} \text{ and } \Psi = e^{-(f_{k-1}(\mathbf{x})-f_{k-1}(\mathbf{y}))^2/2\mu_{(k)}^2}.$$

In a second denoising step the more realistic Rician noise model for DWIs is assumed. The estimated mean values for simplified noise are mapped to the locally varying Rician variance of the DWIs. This heteroscedastic noise is then used in a second filter application (μ –> μ(**x**)) to improve the estimation of the mean DWIs. In addition, the number k of iterations is adapted to the curvature of the DWI images. This averaged DWIs are still biased and need to be corrected further by a BC. Postfiltering is performed also via heteroscedastic noise, which can be modelled by a Taylor expansion of the variance of DTI quantities [9].

C. The bias correction

Within the Rician noise model a bias in the averaged DWIs can be corrected. See in Fig. 2 SNR=DWI_without noise/σ_0 versus MNR= DWI_averaged/σ_0, σ_0 is an asymptotic data driven noise level [9]. The broken curve (C^1) indicates a correction below SNR=0.5, to prevent singularities in DTI quantities caused by the high slope at SNR=0.

Fig. 2 Rician bias correction (solid line) and a modification (broken line) for SNR<0.5.

D. The gold standard model

For validation a small voxel experiment was performed on a consented healthy volunteer. Isotropic 1x1x1 mm^3 DWIs were acquired on a GE 1.5 T MRT scanner using a

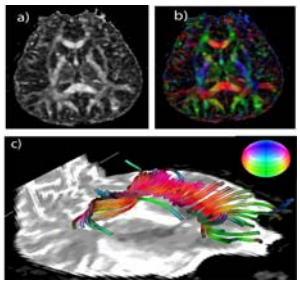

Fig. 3 Gold standard model, panel a) axial FA map, panel b) directional map, panel c) tracks of the corpus callosum.

dual spin echo prepared diffusion sequence; 21 icosahedral gradients and a b-value b=1400 s/mm^2 were applied, a small volume around corpus callosum was measured. Due to the very low averaged SNR~2.2, in addition to our denoising method a median filter and final mask corrections had to be applied to achieve a smooth "realistic" model, which can be used as gold standard.

III. Results

Validation of the denoising method

The denoising method is tested for the diffusion properties mean diffusion (MD), FA and main diffusion direction. Experiments with field strength 3 T, b=1400 s/mm^2 , 21 gradients and NEX=1, 4 and 8 are simulated on the basis of the gold standard model. Negative eigenvalues of the noisy diffusion tensors could be removed completely already for denoising with NEX=1. For quantitative error analysis of diffusion properties noise was put to the model DWIs 100 times, to enable the calculation of the mean squared error (mse) for the ensemble statistics. In Fig. 4 results for MD are presented. Panel a) shows a slice of the model, panel b) the noisy model (NEX=1), and panel c) the ensemble mean after filtering, application of BC and postfiltering (NEX=1). A good agreement between a) and c) is apparent, indicating an essentially unbiased MD average. In panel d) the SNR distribution of the DWIs is presented. In panel e) Box Whisker plots of the relative rooted mse (=1/SNR of MD) for every voxel are shown for NEX=1, 4, 8 after denoising. Left group without BC, right group BC included. Already after full denoising with NEX=1 and BC the SNR of MD is above 50 for 95% of the voxels, this SNR increases with NEX.

In Fig. 5 the same slice is analyzed for FA, panels a-c) like in Fig. 4 but for NEX=4. Again we find an essentially unbiased ensemble mean after denoising with BC. Below,

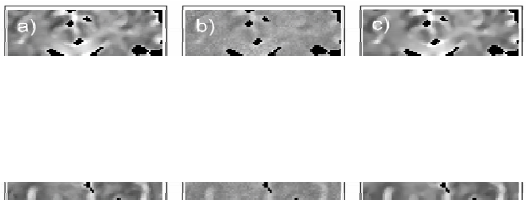

Fig. 4 Error analysis of MD after denoising, see text.

the denoised 1/SNR of FA is presented, in panel d) for NEX=1, in panel e) for NEX=4 and in panel f) for NEX=8. The error situation is less straightforward than in case of MD. NEX=1 produces for white matter only partly a SNR above 25 (green). This improves with NEX=4. For NEX=8 also parts of deep grey matter are well denoised, see for the Thalamus indicated as Th in panel f).

In Fig. 6 the effect of denoising on the main diffusion directions is analyzed. Upper row gives color coded directional maps of the model (a), of one noisy slice (b) and of the ensemble averaged directions after denoising (NEX=8) without postfiltering (c), as a convenient filter for vector fields was not available. Again, the remaining bias is very small, see a) and c). For quantitative error analysis, the ensemble averaged angle between model direction and denoised model direction is presented, before application of BC in the second row, and after application of BC in the last row. Panels d - f) and g - i) are calculated for NEX=(1, 4, 8). In both rows the error is reduced with increasing

Fig. 5 Error analysis of FA after denoising. For panels a-c), see text. Panels d) (NEX=1), e) (NEX=4), f) (NEX=8) present local 1/SNR of FA. Colouring : green < 0.04, blue [0.04, 0.06), red [0.06, 0.08), orange [0.08, 0.1), yellow > 0.1.

Fig. 6 Error analysis of main diffusion directions after denoising, panels a-c) see text. Panels d-i) show mean angular deviations after denoising; colouring : green < 2°, blue [2°, 4°), red [4°, 6°), orange [6°, 8°), yellow > 8°, else see text.

NEX. The error maps resemble those of FA, for NEX=4 and 8 white matter and parts of the Thalamus have a mean angular deviation below 2°. Application of BC improves the error map in high FA regions.

IV. Discussion

Due to patient motion, brain and scanner instabilites scan time (or NEX) is limited. Therefore filtering is needed to fill this gap at least partially. To quantify the effectiveness of our approach, the error maps for simulated voxelwise DWI averaging with NEX= 20, 30, 50 (BC included) were calculated for FA and the main directions. The results are similar to those of panels d-f) in Fig. 5 and panels g-i) of Fig. 6. This corresponds to a gain of scan time by filtering equivalent to NEX= 19, 26 or 42 replications, depending on the actually measured NEX before filtering. In special regions the filter acts differently due to its dependence on the size of the spatial homogeneous regions. So is the filter more effective in the compact genu of corpus callosum and mainly for FA less effective in the thin external capsule.

The human brain data for the gold standard model with 1x1x1 mm^3 resolution and field strength 1.5 T revealed scanner artefacts which could not be removed sufficiently by our method alone. A thorough analysis of the experimental problems with high resolution is beyond our scope. One important restriction for technical parameters like field strength, b-values, voxel size and NEX to measure human brain DTI with small voxels, however, is the need for a reliable quantitative analysis. Our study indicates that experiments with parameters in the range of those applied in section III. could be in this sense reasonable candidates.

V. Conclusion

A numerical denoising method for low SNR DTI is presented. The method is parameterized and validated in a statistically solid way for a human small voxel model. The simulation results indicate the feasibility of standard DTI with smaller voxels than are in use at present, if thermal noise in the DWIs is the source of the dominating DTI artifacts.

VI. References

1. K. Terajima, H. Matsuzawa, K. Tanaka et al (2007) Cell-oriented analysis in vivo using diffusion tensor imaging for normal-appearing brain tissue in multiple sclerosis. NeuroImage 37 : 1278-1285.
2. S.J. Teipel, R. Stahl, O. Dietrich et al (2007) Multivariate network analysis of fiber tract integrity in Alzheimer`s disease. NeuroImage 34 : 985-995.
3. P.J. Basser, D.K. Jones (2002) Diffusion-tensor MRI : theory, experimental design and data analysis – a technical review. NMR. Biomed. 15 : 456-467.
4. S. Basu, T. Fletcher, R. Whitaker (2006) Rician Noise Removal in Diffusion Tensor MRI, Proc MICCAI 2006, Springer, 117-125.
5. P. Fillard, V. Arsigny, X. Pennec, N et al (2006) Clinical DT-MRI estimation, smoothing and fiber tracking with log-Euclidian metrics, in: Proc. Third IEEE International Symposium on Biomedical Imaging, 786-789.
6. X. Zhang, H. Ye, H. Zhang (2008) Multi-Channel Wavelet-Based Diffusion Method for Denoising DTI Images, in: Proceedings of International Conference on Biomedical Engineering and Information, 178-182.
7. M. Martin-Fernandez, E. Munzo-Moreno, L. Cammoun et al (2009) Sequential Anisotropic Multichannel Wiener Filtering with Rician Bias Correction Applied to 3D Regularization of DWI Data, Medical Image Analysis 13/1, 19-35.
8. K.R. Hahn, S. Prigarin, K.M. Hasan (2005) The Feasibility of Diffusion Tensor Imaging for the Human Brain at 1 mm^3 Resolution, in: Proceedings of the 13th Annual Meeting of the ISMRM, Miami, pp. 161.
9. K. R. Hahn, S. Prigarin, K. Rodenacker et al (2009) Denoising for Diffusion Tensor Imaging with low Signal to Noise Ratios : Method and Monte Carlo Validation, International Journal of Biomathematics and Biostatistics, in press.
10. G. Winkler, V. Aurich, K. R. Hahn et al (1999) Noise reduction in images : some recent edge-preserving methods, J. Patt Recog Image Analysis 9/4, 749-766.

Author: Klaus R. Hahn
Institute: Institute of Biomathematics & Biometry, HMGU
Street: Ingolstaedter Landstr. 1
City: D-85764 Neuherberg
Country: Germany
Email: hahn@gsf.de